

# Coupled Noise Estimation for Distributed RC Interconnect Model

Janet M. Wang, Qingjian Yu and Ernest S. Kuh  
 University of California at Berkeley  
 Berkeley CA 94720, U.S.A  
 kuh@eecs.berkeley.edu, wml@eecs.berkeley.edu

## Abstract

With the increase in signal speed and the development of process technology, distributed RC line model is found to be more suitable for on-chip interconnects than lumped RC model, especially for interconnects around and below  $0.25\mu\text{m}$ . In this paper, we first describe a new explicit form for crosstalk approximation for coupled RC lines. Then we introduce a novel passive model order reduction technique for distributed RC lines. These two parts serve as two steps in static noise analysis of full on-chip interconnect networks which are called pruning process and static analysis process.

## 1 Introduction

As processor cycle times become shorter and chips become larger and more complex, noise analysis and crosstalk avoidance become more important. Various transient analysis techniques based on linear model reduction techniques [1][2] have been used to estimate noise[3]. These model reduction techniques help in reducing the computational cost, however they are only suitable for lumped RC or RLC interconnect model. It is shown in [4] that due to the fast rise time and narrow line width, distributed properties of on-chip wiring need to be taken into account. The traditional lumped-circuit RC representation is no longer adequate since it substantially underestimates both crosstalk and delay. This paper is organized as follows. In section 2, we provide an explicit form of coupled RC lines. In section 3, we introduce the new model order reduction technique. In section 4, we give some examples and make conclusions, respectively.

## 2 Explicit Form for Crosstalk Estimation of RC lines

### 2.1 A Moment-based Single RC line Model

With the assumption of TEM mode of wave propagation, the distribution of voltages and currents along  $m$  parallel uniform RC lines can be described in the frequency domain by the Telegraph equations:

$$\frac{\partial V(z, s)}{\partial z} = -RI(z, s) \quad (1)$$

$$\frac{\partial I(z, s)}{\partial z} = -sCV(z, s) \quad (2)$$

where  $R$  is the per unit length (p.u.l) resistance matrix and  $C$  is the p.u.l capacitance matrix. For two capacitively coupled RC lines, rewriting (1) and (2) in the time domain yields

$$\frac{1}{r_1} \frac{\partial^2 v_1}{\partial z^2} = (c_1 + c_c) \frac{\partial v_1}{\partial t} - c_c \frac{\partial v_2}{\partial t} \quad (3)$$

$$\frac{1}{r_2} \frac{\partial^2 v_2}{\partial z^2} = (c_2 + c_c) \frac{\partial v_2}{\partial t} - c_c \frac{\partial v_1}{\partial t} \quad (4)$$

where  $r_1$  ( $r_2$ ) and  $c_1$  ( $c_2$ ) are p.u.l resistance and capacitance of line 1 (2) respectively.  $c_c$  denotes the p.u.l coupling capacitance between the two RC lines.  $v_1$  ( $v_2$ ) represents the voltage along line 1 (2). From (3) and (4), the distribution of voltage along a single RC line without coupling in the time domain can be written as:

$$\frac{1}{r} \frac{\partial^2 v(z, t)}{\partial z^2} = c \frac{\partial v(z, t)}{\partial t} \quad (5)$$

where  $r$  and  $c$  are per unit length resistance and capacitance of the line. Suppose  $R_s$  is the applied voltage source resistance and  $C_{load}$  is the load capacitance. By using Taylor series expansion at  $s = 0$  and comparing the coefficients of the same  $s$  terms, we result in a recursive moment generation process. For the  $i$ th moments,

$$I^i(d, 0) = C_{load} V^{i-1}(d, 0)$$

$$I^i(0, 0) = \int_0^d c V^{i-1}(z, 0) dz + I^{i-1}(d, 0)$$

$$V_s^i(0) - V^i(0, 0) = R_s I^i(0, 0)$$

and

$$V^i(x, 0) = V^i(0, 0) - \int_0^x r \left( \int_y^d c V^{i-1}(z, 0) dz + I^i(d, 0) \right) dy$$

If the input of the RC line is a unit  $\delta(t)$  function, it is obvious that  $V^1(0, 0)$  and  $V^1(d, 0)$  are negative. And it can be shown easily that  $V^2(d, 0)$  is positive. Thus, the transfer function of the line can be written as:

$$\begin{aligned} H(s) &= \frac{V(d, s)}{V_{in}(s)} = V^0(d, 0) + V^1(d, 0)s + V^2(d, 0)s^2 + \dots \\ &\approx \frac{a_1 s + a_0}{s + b_0} \end{aligned}$$

By Pade approximation, we have

$$b_0 = -\frac{V^1(d, 0)}{V^2(d, 0)} \quad (6)$$

while  $a_0 = V^0(d, 0)b_0$  and  $a_1 = V^0(d, 0) - V^1(d, 0)b_0$ .

*Theorem 1* This moment-based model is stable .  
proof:

Since  $V^1(d, 0) < 0$  and  $V^2(d, 0) > 0$ ,  $b_0$  is nonnegative. Thus the single pole  $s_1 = -b_0 \leq 0$  shows that the model is stable.  $\square$

In the time domain, if the input is a normalized step function,

$$v(d, t) = \frac{a_0}{b_0} + K_1 e^{-b_0 t} \quad (7)$$

where

$$K_1 = -\frac{a_0 - a_1 b_0}{b_0} \quad (8)$$

## 2.2 Explicit Form for Crosstalk Estimation

Assume we have two identical coupled RC lines. By introducing new variables  $v^+$  and  $v^-$ , from equation ( 3) and (4), we have two decoupled equations:

$$\frac{\partial^2 v_+}{\partial x^2} = rc \frac{\partial v_+}{\partial t} \quad (9)$$

$$\frac{\partial^2 v_-}{\partial x^2} = r(c + 2c_c) \frac{\partial v_-}{\partial t} \quad (10)$$

In the case the source resistance and the load capacitance of line 1 and 2 are the same, after decoupling, the source resistance and the load capacitance of line 1' and 2' are still the same and equal to those before decoupling. Moreover, each of equations (9) and (10) has the same form as ( 5). Thus, we can get the explicit expression of  $v_+$  and  $v_-$  by the similar recursive moment derivation process. Changing back into  $v_1$  and  $v_2$  yields

$$v_1(d, t) = E_1 + 1/2(K_{11}(E_1 + E_2)exp(-b_{01}t) + K_{12}(E_1 - E_2)exp(-b_{02}t)) \quad (11)$$

$$v_2(d, t) = E_2 + 1/2(K_{11}(E_1 + E_2)exp(-b_{01}t) - K_{12}(E_1 - E_2)exp(-b_{02}t)) \quad (12)$$

where  $E_1$  and  $E_2$  are steady states of voltage sources at the near ends of both RC lines,  $K_{11}$  and  $K_{12}$  are obtained by equation (8), and  $b_{01}$  and  $b_{02}$  by (6). If  $E_2 = 0$ , then the peak value of  $v_2(d, t)$  is the maximum noise induced by the capacitive coupling which can be evaluated by  $v_p = v_2(d, t_p) = \frac{1}{2}(K_{11}E_1 exp(-b_{01}t_p) - K_{12}E_1 exp(-b_{02}t_p))$  where  $t_p = \frac{1}{b_{01} - b_{02}} \log(\frac{b_{01}}{b_{02}})$ . This moment-based model is simple and efficient. It only depends on the first three moments of the voltages along the RC lines. Moreover, it can be easily extended to cases with ramp input functions and for cases with different RC lines coupled together as well as with different source resistors or load capacitors[8]. In our pruning engine, this model serves as "watchman" that can identify dangerous clusters which have high coupled noise. These clusters will then be sent to static noise analysis process for detailed checking. At the end of static noise analysis process, noise report and timing deterioration report for a certain cluster will be generated. However, due to its simplicity, for

cases when a victim couples with several aggressors, shifting and superposition techniques are applied to sum up the maximum noise value caused by each aggressor. In this way, we obtain a rough estimation of the worst case coupled noise for each victim. And the estimation thus generated can be too pessimistic. A more accurate model is needed for static noise analysis process. In the next section, a new model is presented to meet this requirement.

## 3 Passive Model Order Reduction Technique for RC Lines

In this section, we introduce a novel model for distributed RC lines. This model is proved to be passive and preserves moments. Furthermore, it shows very good accuracy and efficiency from the experiment results. We adopt this model in our static noise analysis process.

The basic differential equations governing m coupled RC lines are ( 1) and (2). According to [6],  $C$  matrix in ( 2) is positive definite.

Let

$$\tilde{V}(z, s) = R^{-\frac{1}{2}} V(z, s) \quad (13)$$

$$\tilde{I}(z, s) = R^{\frac{1}{2}} I(z, s) \quad (14)$$

Substituting (13) and (14) into (1) and (2), we obtain

$$\frac{\partial \tilde{V}(z, s)}{\partial z} = -\tilde{I}(z, s) \quad (15)$$

$$\frac{\partial \tilde{I}(z, s)}{\partial z} = -s A \tilde{V}(z, s) \quad (16)$$

where

$$A = R^{\frac{1}{2}} C R^{\frac{1}{2}} \quad (17)$$

$\tilde{V}(z, s)$  is a continuous function with  $z$  varying from 0 to  $d$ , and  $s$  from 0 to  $\infty$ .

*Theorem 2* We can construct a transform  $U(z)$  so that  $\hat{V}(z, s)$  can be approximated as

$$\tilde{V}(z, s) \approx \hat{V}(z, s) = U(z)x(s) \quad (18)$$

where  $U(z)$  only depends on  $z$  and  $x(s)$  is a function vector which only depends on  $s$ .

proof: Since  $\tilde{V}(z, s)$  can be expanded as Taylor series near any point  $s_0$ ,

$$\begin{aligned} \tilde{V}(z, s) &= \tilde{V}^0(z, s_0) + \tilde{V}^1(z, s_0)(s - s_0) + \dots \\ &\quad + \frac{\tilde{V}^{i-1}(z, s_0)}{(i-1)!} (s - s_0)^{i-1} + \dots \\ &= \sum_{i=0}^{n-1} \frac{\tilde{V}^i(z, s_0)}{i!} (s - s_0)^i + \mathcal{O}((s - s_0)^n) \end{aligned}$$

where

$$\tilde{V}^i(z, s_0) = \left. \frac{\partial^i \tilde{V}(z, s)}{\partial s^i} \right|_{s=s_0}$$

We use  $H_b(z)$  to denote the first n-moment subspace  $span\{\tilde{V}^0(z, s_0), \tilde{V}^1(z, s_0), \dots, \tilde{V}^{n-1}(z, s_0)\}$ . Suppose a basis of  $H_b(z)$  subspace is  $\{u_0(z), u_1(z), \dots, u_{k-1}(z)\}$ . Let  $H_{b\infty}(z)$  be defined as  $span\{\tilde{V}^0(z, s_0), \tilde{V}^1(z, s_0), \dots, \tilde{V}^{n-1}(z, s_0), \tilde{V}^n(z, s_0), \dots\}$  which is an infinite-dimensional space. Suppose a basis for this space is  $\{u_0(z), u_1(z), \dots, u_{k-1}(z), \dots, u_{\bar{k}}(z)\}$  where  $\bar{k}$  is the total number of orthogonal normal vectors and it can be as

large as  $\infty$ . Then we have two scenarios:

when  $0 \leq i \leq n-1$ ,  $\tilde{V}^i(z, s_0) = \sum_{j=0}^{k-1} a_{ij} u_j(z)$

when  $i \geq n$ ,  $\tilde{V}^i(z, s_0) = \sum_{j=0}^{k-1} a_{ij} u_j(z) + \sum_{j=k}^{\bar{k}} a_{ij} u_j(z)$

hence, if we only consider the terms depending on the basis  $\{u_0(z), u_1(z), \dots, u_{k-1}(z)\}$ , we can approximate  $\tilde{V}(z, s)$  as

$$\begin{aligned} \tilde{V}(z, s) &\approx \hat{V}(z, s) = \sum_{j=0}^{k-1} a_{0j} u_j(z) + \sum_{j=0}^{k-1} a_{1j} u_j(z) (s - s_0) + \dots \\ &+ \sum_{j=0}^{k-1} a_{n-1,j} u_j(z) (s - s_0)^{n-1} + \dots = \sum_{i=0}^{\infty} \sum_{j=0}^{k-1} a_{ij} u_j(z) (s - s_0)^i \end{aligned}$$

Rearranging the terms, we have  $\tilde{V}(z, s) \approx \hat{V}(z, s) = U(z)x(s)$  where  $U(z) = [u_0(z), u_1(z), \dots, u_{k-1}(z)]$

$$x(s) =$$

$$\begin{bmatrix} a_{0,0} + \dots + a_{n-1,0} (s - s_0)^{n-1} + \sum_{i=0}^{\infty} a_{i,0} (s - s_0)^i \\ a_{0,1} + \dots + a_{n-1,1} (s - s_0)^{n-1} + \sum_{i=n}^{\infty} a_{i,1} (s - s_0)^i \\ \dots \\ a_{0,k-1} + \dots + a_{n-1,k-1} (s - s_0)^{n-1} + \sum_{i=n}^{\infty} a_{i,k-1} (s - s_0)^i \end{bmatrix}$$

Since  $k \ll \bar{k}$ , we manage to reduce the original infinite dimension system to a  $k$ -dimension system.  $\square$

It can be shown by the definition from [7] that  $U(z)$  represents an  $L^2$  Hilbert space. The construction of  $U(z)$  is included in section 3.1. Here, we assume that  $U(z)$  is known.

Replacing  $\hat{V}(z, s)$  in (15) with (18) yields

$$\frac{\partial \hat{V}(z, s)}{\partial z} = -\hat{I}(z, s) \quad (19)$$

$$\frac{\partial \hat{I}(z, s)}{\partial z} = -sA\hat{V}(z, s) \quad (20)$$

It is quite easy to show that  $\hat{I}(z, s)$  matches the first  $n$  moments of  $\tilde{I}(z, s)$ . So, we have

*Theorem 3* This reduced-order model preserves the moments. Since

$$\hat{I}(z, s) = -\frac{dU(z)}{dz} x(s) \quad (21)$$

differentiating both sides of (21) with respect to variable  $z$  and substituting (21) into (16) give

$$\frac{d^2 U(z)}{dz^2} x(s) = sAU(z)x(s) \quad (22)$$

Multiplying  $U^T(z)$  on both sides of (22) and integrating with respect to  $z$  from 0 to  $d$ , it follows

$$\left( \int_0^d U^T(z) \frac{d^2 U(z)}{dz^2} dz \right) x(s) = \left( s \int_0^d U^T(z) AU(z) dz \right) x(s) \quad (23)$$

Let

$$M = \int_0^d U^T(z) AU(z) dz \quad (24)$$

where  $M$  is positive definite provided that  $U(z)$  is of full rank.

By using integration by parts, the l.h.s. of (23) becomes:

$$\left( \int_0^d U^T(z) \frac{d^2 U(z)}{dz^2} dz \right) x(s) = \left( U^T(z) \frac{dU(z)}{dz} \Big|_0^d \right) x(s)$$

$$- \left( \int_0^d \frac{dU^T(z)}{dz} \frac{dU(z)}{dz} dz \right) x(s) \quad (25)$$

Let

$$N = \int_0^d \frac{dU^T(z)}{dz} \frac{dU(z)}{dz} dz \quad (26)$$

It is obvious that  $N$  is nonnegative definite. Moreover, if there exists a nonzero length region  $[z_1, z_2] \in [0, d]$  such that matrix  $\frac{dU(z)}{dz}$  is of full rank, then  $N$  is positive definite. We combine the first term on the r.h.s. of (25) with the boundary conditions. Note that from (21),  $\frac{dU(z)}{dz} \Big|_{z=0} x(s) = -\hat{I}(0, s)$  and  $\frac{dU(z)}{dz} \Big|_{z=d} x(s) = -\hat{I}(d, s)$ . Therefore,

$$\left( U^T(z) \frac{dU(z)}{dz} \Big|_0^d \right) x(s) = U^T(0)\hat{I}(0, s) - U^T(d)\hat{I}(d, s)$$

$$= \begin{bmatrix} U(0) \\ U(d) \end{bmatrix}^T \hat{I}_s(s)$$

where  $\hat{I}_s = \begin{bmatrix} \hat{I}(0, s) \\ -\hat{I}(d, s) \end{bmatrix}$ . Thus, the state equations of the reduced order model can be written in the frequency domain as

$$(sM + N)x(s) = \tilde{B}\hat{I}_s \quad (27)$$

where

$$\tilde{B} = \begin{bmatrix} U(0) \\ U(d) \end{bmatrix}^T \quad (28)$$

Assume the output equations of the system are

$$y = \begin{bmatrix} \hat{V}(0) \\ \hat{V}(d) \end{bmatrix} = \begin{bmatrix} U(0) \\ U(d) \end{bmatrix} x(s) = \tilde{B}^T x(s) \quad (29)$$

Then, the input impedance matrix of the system will be

$$Z(s) = \tilde{B}^T (sM + N)^{-1} \tilde{B} \quad (30)$$

*Theorem 4* This reduced-order model preserves passivity. proof:

For all complex  $s$ ,

$$Z(s^*) = Z^*(s) \quad (31)$$

where  $*$  is the complex conjugate operator.

For any column vector  $x$ ,

$$\begin{aligned} x^{*T} (Z(s) + Z^*(s)^T) x &= x^{*T} \tilde{B}^T (sM + N)^{-1} [(sM + N) \\ &+ (s^*M + N)^T] (sM + N)^{-T} \tilde{B} x \end{aligned} \quad (32)$$

Let

$$\hat{x} = (sM + N)^{-T} \tilde{B} x \quad (33)$$

and  $s = \sigma + j\omega$ . Inserting (33) in (32) results in

$$x^{*T} (Z(s) + Z^*(s)^T) x = \hat{x}^{*T} [N + N^T + \sigma(M + M^T)] \hat{x} \quad (34)$$

From (24) and (26),  $M, N$  are positive definite matrices. Therefore, if  $\sigma > 0$ ,

$$x^{*T} (Z(s) + Z^*(s)^T) x > 0 \quad (35)$$

$\square$

This idea can be easily extended to general RLGC transmission line cases[8]. Note that in RC line cases both matrices  $M$  and  $N$  are symmetric. This fact allows us to lower the matching order by half compared with general RLGC transmission line cases when achieving the same level accuracy.

### 3.1 Moments and $U(z)$ Generation

Unlike Lanczos and Arnoldi algorithms, in our method, moments construct an  $L^2[0, d]$  Hilbert space. By applying Modified Gram-Schmit algorithm, a basis for this Hilbert space is found which in turn forms the column vectors in  $U(z)$ .

Expanding  $\hat{V}(z, s)$  and  $\hat{I}(z, s)$  as Taylor series near  $s = s_k$ , we get

$$\hat{V}(z, s) = \hat{V}^0(z, s_k) + \hat{V}^1(z, s_k)(s - s_k) + \hat{V}^2(z, s_k)(s - s_k)^2 \dots \quad (36)$$

$$\hat{I}(z, s) = \hat{I}^0(z, s_k) + \hat{I}^1(z, s_k)(s - s_k) + \hat{I}^2(z, s_k)(s - s_k)^2 \dots \quad (37)$$

Combined with (15) and (16), it gives

$$\frac{\partial \hat{V}^i(z, s_k)}{\partial z} = -\hat{I}^i(z, s_k) \quad (38)$$

$$\frac{\partial \hat{I}^i(z, s_k)}{\partial z} = -s_k A \hat{V}^i(z, s_k) - A \hat{V}^{i-1}(z, s_k) \quad (39)$$

The solution to (38) and (39) is :

$$\begin{bmatrix} \hat{V}^i(z, s_k) \\ \hat{I}^i(z, s_k) \end{bmatrix} = e^{-Bz} \begin{bmatrix} \hat{V}^i(0, s_k) \\ \hat{I}^i(0, s_k) \end{bmatrix} + e^{-Bz} \int_0^z e^{Bz'} \begin{bmatrix} 0 & 0 \\ -A & 0 \end{bmatrix} \begin{bmatrix} \hat{V}^{i-1}(z', s_k) \\ \hat{I}^{i-1}(z', s_k) \end{bmatrix} dz' \quad (40)$$

where  $B = \begin{bmatrix} 0 & -I \\ -s_0 A & 0 \end{bmatrix}$  and  $i = 1, 2, \dots$

By recursively using (40), we can get higher order moments for  $\hat{V}(z, s)$  and  $\hat{I}(z, s)$ . It is easy to see that  $\begin{bmatrix} \hat{V}^i(z, s_k) \\ \hat{I}^i(z, s_k) \end{bmatrix}$  can be expressed as the sum of exponential functions of  $z$ , which in turn can be easily expanded into polynomials. Hence, though we have integral operator in our formulation, we use explicit calculation to evaluate the integral instead of using trapezoidal or other numerical integration methods. As shown in section 4, for each expansion point, the moment matching order can be as low as two, which we have found to be adequate for accurate results.

Now the question left in this section is to show how to construct  $U(z)$ . Generally, for  $n$  multiple expansion point cases, if we calculate up to  $k_j$  moments at  $j$ th point, where  $j = 0, 1, \dots, n$ , the  $L^2$  Hilbert space can be written as:

$$H_b(z) = \text{span}\{\hat{V}^0(z, s_0), \hat{V}^1(z, s_0), \dots, \hat{V}^{k_0}(z, s_0), \hat{V}^0(z, s_1), \hat{V}^1(z, s_1), \dots, \hat{V}^{k_1}(z, s_1), \dots, \hat{V}^0(z, s_n), \hat{V}^1(z, s_n), \dots, \hat{V}^{k_n}(z, s_n)\}$$

An orthogonal basis can be found by the Modified Gram-Schmidt algorithm for  $L^2$  Hilbert space as follows:

```

for i = 1 to m
/* m is the total number of columns in  $H_b(z)$  */
 $q_i = V_i$  /* the  $i$ th column vector in  $V(z)$  */
for j = 1 to i - 1
/* subtract component in  $q_j$ 
direction from  $V_i$  */
 $r_{ij} = \int_0^d q_j(z)^T q_i(z) dz$ 
 $q_i = q_i - r_{ij} q_j$ 
end for

```

```

 $r_{ii} = \sqrt{\int_0^d q_i^T(z) q_i(z) dz}$ 
if  $r_{ii} = 0$  /* deflation happens */
quit
end if
 $q_i = q_i / r_{ii}$ 
end for

```

In cases when  $s_i$  is complex, the above algorithm should be implemented twice for the real and imaginary part of the vector  $q_i$  respectively so that we can obtain a real transformation matrix  $U(z)$ .

## 4 Experiment Results

In Example 1, we have a single RC line with driver resistance much bigger than the line resistance. Fig. 1 shows the waveform at the far end of the line. It is easy to see that SPICE, Sakurai's method[5] and our new explicit form match well. Example 2 has driver resistance smaller than the line resistance. In Fig. 2, SPICE and our new explicit form have very close results, whereas Sakurai's method has an error as high as 50%. Under  $0.45\mu m$  technology, we have three coupled RC lines as in Fig.3. The middle one is victim. In Example 3, the victim has no input signal while two aggressors have pulse input signals with the same switching direction. Referring to Fig.4, we can see that our result matches well with distributed model by SPICE, but the lumped RC model has lower noise peak and smaller noise width and produces an error around 20%. In Example 4, under similar circumstances as in Example 3, if  $0.25\mu m$  lines are used, the victim tends to have higher noise peak and wider noise width (refer to Fig. 5). In Example 3 and 4, we select two expansion points:  $1 \times 10^{-7}$  as the one near  $s = 0$  and  $3 \times 10^9$  as the one near infinity. At each expansion point, we match the moments to the 2nd order. According to the line parameters under different technologies based on SIA National Technology Roadmap, Table 1. lists the noise peak (column 3) and noise width (column 4) generated by the new passive model with different technology generation (column 1) and different line length (column 2). The error rate in column 5 is the error of noise peak with respect to the results by SPICE, and in column 6 the error rate is of noise width with respect to SPICE. As shown in the Table, with the decreasing of the technology generation and increasing of the line length, we have higher noise peak and wider noise width. As we know, from  $0.25\mu m$  to  $0.07\mu m$ , the driver resistance and  $V_{dd}$  have the trend to decrease, thus we have more serious noise problem with smaller line widths. Furthermore, notice the changing of the line length and noise, it seems that lines with length  $\geq 1mm$  are more likely to be "noisy" lines than shorter ones.

## 5 Conclusions

We have presented a new explicit form for coupled RC lines and a novel algorithm for passive model order reduction with multipoint moment matching for distributed interconnect networks. They are used in static noise analysis for on-chip interconnect networks. Moreover, these models can also be useful to general RLGC interconnect networks.

## Reference

[1] P.Feldmann and R.W.Freund, "Reduced-order modeling of large linear subcircuits via a block Lanczos algorithm," Proc. of DAC'95, pp.474-479, June 1995.

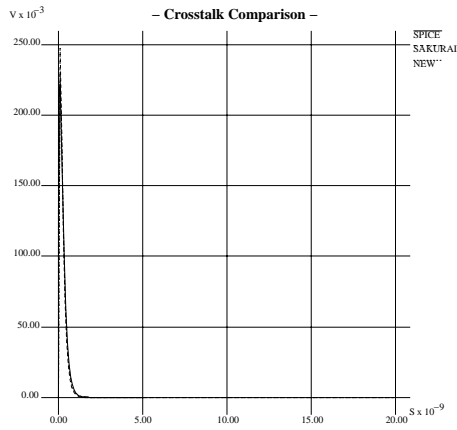


Figure 1:

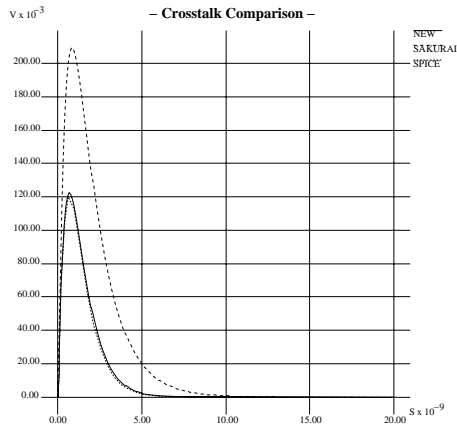


Figure 2:

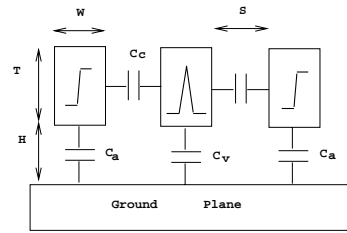


Figure 3:

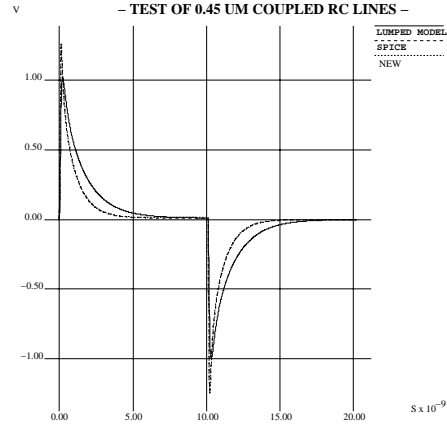


Figure 4:

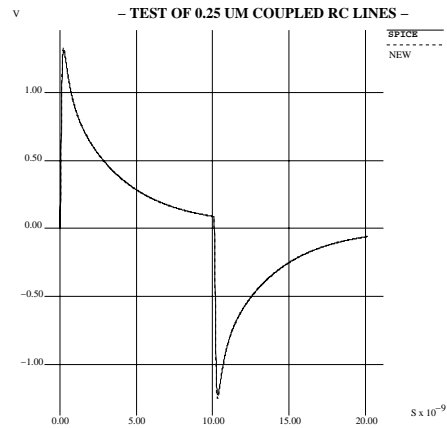


Figure 5:

[2] A.Odabasioglu, M.Celik and L.T.Pileggi, "PRIMA: passive reduced-order interconnect macromodeling algorithm," Proc. IC-CAD'97, pp. 58-65, Nov. 1997.  
 [3] K.Shepard, V.Narayanan etl, "Global Harmony: Coupled Noise Analysis for Full-Chip RC interconnect Networks", in ICCAD 1997, p147-151  
 [4] A.Deutsch, et, "When are transmission-line effects important for on-chip interconnections?", IEEE Trans. on MTT, vol.45, pp.1836-1844, October 1997.  
 [5] T. Sakurai, "Closed-Form Expressions for Interconnection Delay Coupling, and Cross talk in VLSI's", IEEE Transactions on Electron Devices, Vol. 40. No. 1. January  
 [6] F.Y.Chang, "Transient Analysis of lossless Coupled Transmission lines in a nonhomogeneous dielectric medium", in IEEE Trans. on MTT, Vol. 18, No. 9 1971.  
 [7] S.Berberian, Introduction to Hilbert Space. 1976  
 [8] J.M.Wang, Q.J.Yu and E.S.Kuh, "Coupled noise analysis for distributed interconnects", ERL Memorandum, M98/14, 1998

Table 1: Noise Report

| Tech ( $\mu m$ ) | d (mm) | peak (v) | width (ns) | PErr (%) | WErr (%) |
|------------------|--------|----------|------------|----------|----------|
| 0.25             | 0.1    | 0.058    | 0.6        | 3.1      | 2.4      |
|                  | 1      | 0.198    | 0.79       | 0.8      | 1.3      |
|                  | 10     | 0.247    | 1.42       | 0.5      | 3.2      |
| 0.18             | 0.1    | 0.078    | 0.5        | 2.9      | 5.3      |
|                  | 1      | 0.213    | 1.21       | 0.3      | 4.7      |
|                  | 10     | 0.351    | 1.78       | 2.2      | 1.5      |
| 0.13             | 0.1    | 0.134    | 1.18       | 0.9      | 1.3      |
|                  | 1      | 0.679    | 1.80       | 1.7      | 0.9      |
|                  | 10     | 0.933    | 2.40       | 0.1      | 4.0      |
| 0.07             | 0.1    | 0.337    | 1.09       | 2.7      | 2.1      |
|                  | 1      | 0.781    | 3.45       | 3.2      | 3.7      |
|                  | 10     | 0.823    | 5.31       | 1.5      | 5.5      |